Theory of collisionally aided radiative excitation

S. Yeh and P. R. Berman
Department of Physics, New York University, New York, New York 10003
(Received 18 September 1978)

The excitation of a two-level active atom by a radiation field in the presence of a low-density perturber bath is studied. In particular, the collisional enhancement of the absorption cross section is investigated. Features of the absorption-line profiles are predicted on physical grounds using a dressed-atom approach and verified by detailed numerical calculations for attractive, repulsive, and Lennard-Jones-type interatomic potentials. Complete spectra of the absorption cross section both as a function of detuning and as a function of field strength are given. In the weak-field limit, the results are compared with those of traditional pressure-broadening theory and to the recent experimental results of Carlsten *et al.* In the strong-field limit, the results display a saturation behavior consistent with the predictions of Lisitsa and Yakovlenko.

I. INTRODUCTION

With the development of high-intensity laser sources, there has been renewed interest in the study of atomic collisions in the presence of radiation fields.[1-15] Both collisionally aided radiative excitation (or emission) (CARE), sometimes referred to as "optical collisions,"[1-3] and radiatively aided inelastic collisions (RAIC), sometimes referred to as "radiative collisions,"[5-10] have been examined by a number of authors. The discussion in this paper is limited to CARE although RAIC can be studied by the same methodology to be presented here.

To put the CARE problem into some perspective, consider a two-level active atom with level separation ω_0 subjected to an applied radiation field of frequency ω. The active atoms also undergo collisions with structureless perturbers at some rate Γ and one wishes to calculate the absorption cross section as a function of detuning $\Delta = \omega - \omega_0$. The field amplitude E in frequency units is given by $\chi = \mu E/2\hbar$, where μ is the dipole-moment matrix element of the transition.

If the detuning is greater than both the Doppler width and power-broadened homogeneous width, i.e., $|\Delta|$>Doppler width $\gtrsim\chi$, the absorption cross section is negligible in the absence of collisions and can be enhanced by collisional processes. Consequently, the study of CARE is restricted to detunings $|\Delta|$>Doppler width $\approx 10^{10}$ sec^{-1}. In situations where lasers with limited tunability are employed so that large $|\Delta|$ can not be avoided, CARE may provide a means for increasing the absorption of the sample.

The case of large field strengths $\chi > |\Delta| > 10^{10}$ sec^{-1} requires some additional discussion. Such field strengths can be attained only with pulsed lasers. For pulse rise times longer than $|\Delta|^{-1} \lesssim 10^{-10}$ sec the atomic excitation would adiabatically follow the field in the absence of collisions, and the atom would return to its ground state following[16] the pulse. However, collisions interfere with the adiabatic following and give rise to some net absorption following the radiation pulse. In this limit, collisions are essential for absorption to occur. On the other hand CARE is less important if the pulse rise time is faster than $|\Delta|^{-1}$ since, in this limit, there can be substantial absorption in the absence of collisions.

Thus, the conditions of interest for CARE are

$$|\Delta| > \text{Doppler width} \gtrsim \chi \tag{1a}$$

or

$$\chi > |\Delta| > \text{Doppler width, and radiation pulse rise time} > |\Delta|^{-1}. \tag{1b}$$

For the remainder of this paper we assume that condition (1a) or (1b) is satisfied although the calculations presented in Secs. III and IV isolate the CARE contribution to the absorption even if these conditions do not hold.

If conditions (1) are satisfied, the atomic dipole oscillates with a period $\tau \lesssim |\Delta|^{-1} < 10^{-10}$ sec in a reference frame rotating at frequency ω_0. Thus the time scale of importance in the problem is $\tau \lesssim 10^{-10}$ sec—any processes slower than that can not cancel the rapid oscillation of the dipole. It is assumed that $\Gamma \ll |\Delta|$, i.e., the perturber density is such that at most one collision occurs in the interval τ (typically, valid for pressures <1.0 atm). The condition $\Gamma \ll |\Delta|$ is equivalent to taking the CARE rate to be linear in the perturber density. One can calculate the CARE contribution for a single collision and than average over all possible collisions to obtain the CARE rate.

In the limit of weak fields [Eq. (1a)], the study of CARE is essentially that of pressure-broadened linear absorption. This area of research enjoys

a long history,[17-23] but there are few papers that present detailed numerical calculations for the entire range of detuning, although asymptotic formulas are available in various limits.[18-21] For strong fields, there have been some numerical studies of radiatively aided inelastic collisions,[2,3,5,6] but most of these calculations have concentrated on obtaining analytical approximations for various limits of detunings and field strengths. Moreover, most strong-field CARE and RAIC calculations have utilized somewhat unphysical potentials, i.e., of the form $-|c|/R^n$.

It is our purpose to present a physical picture of CARE for attractive, repulsive, and Lennard-Jones-type interatomic potentials. General features of the results are predicted on the basis of simple physical arguments and detailed numerical calculations are presented to verify the predictions. This paper also forms the basis for future work that will consider level schemes more complicated than the two-level systems discussed below.

II. GENERAL CONSIDERATIONS

Consider a collision between a two-level active atom and a ground-state perturber. The active atom's energy levels are shifted during a collision and this shift is shown schematically in Fig. 1 for some specific collision impact parameter b and relative velocity v. The shift of level 2 relative to level 1 determines whether collisions increase or decrease the 1-2 transition frequency relative to its unperturbed value ω_0. In the case shown, the frequency shift is towards the red and one speaks of an attractive (relative) potential. Conversely, for a relative shift towards the blue, one speaks of a repulsive potential. Collision energies are assumed to be larger than the detuning $|\Delta|$, but not sufficient to couple the levels in the absence of applied fields. (We have set $\hbar = 1$ and measure energy in frequency units.)

If, for some t during the collision, the instantaneous transition frequency $\omega_0(t)$ equals the frequency of the applied field, there is an "instantaneous resonance" for this interaction. For the case shown in Fig. 1, "instantaneous resonances" occur for a range of red detunings, but not for any blue detunings. As is described below, the presence of instantaneous resonances can greatly enhance the absorption cross section, especially in the case of large detunings.

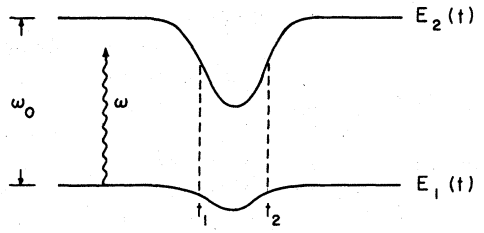

FIG. 1. Variation of the atomic energy levels $E_1(t)$, $E_2(t)$ of a two-level atom during a collision in the classical-field picture for an attractive potential. For the incident field frequency ω shown, instantaneous resonances occur at times t_1 and t_2 during the collision. Note that instantaneous resonances occur for a range of $\Delta = \omega - \omega_0 < 0$ but not if $\Delta > 0$.

The picture presented above is best used when the applied radiation fields are weak. For the case of strong external fields, a dressed-atom[24] approach provides additional insight. The dressed-atom approach can be used for weak as well as strong external fields. In this approach, the unperturbed Hamiltonian H_0 is taken to consist of the free atomic Hamiltonian + free-field Hamiltonian + atom-field interaction. In the absence of spontaneous emission, and in the rotating-wave approximation, the two dressed states (eigenstates of H_0) are the linear combinations of the two bare states $|1,n\rangle$, $|2,n-1\rangle$, given by

$$|\mathrm{I}\rangle = \frac{1}{\sqrt{2}}\left(1+\frac{\Delta}{\Omega}\right)^{1/2}|1,n\rangle + \frac{1}{\sqrt{2}}\left(1-\frac{\Delta}{\Omega}\right)^{1/2}|2,n-1\rangle\,,$$

$$|\mathrm{II}\rangle = \frac{1}{\sqrt{2}}\left(1-\frac{\Delta}{\Omega}\right)^{1/2}|1,n\rangle - \frac{1}{\sqrt{2}}\left(1+\frac{\Delta}{\Omega}\right)^{1/2}|2,n-1\rangle\,, \tag{2}$$

where the bare states are labeled by both the field and atomic variables with n being the number of photons in the field and

$$\Omega = (\Delta^2 + 4\chi^2)^{1/2}$$

is the Rabi frequency with χ the field strength in frequency units. The energies of these eigenstates are

$$E_{\mathrm{I}} = E_1 + n\omega - \tfrac{1}{2}\Delta \pm \tfrac{1}{2}\Omega\,,$$
$$E_{\mathrm{II}} = E_1 + n\omega - \tfrac{1}{2}\Delta \mp \tfrac{1}{2}\Omega\,; \tag{3}$$

the upper signs are used for positive Δ and the lower signs for negative Δ so that

$$E_{\mathrm{II}} - E_{\mathrm{I}} = \mp\Omega\,. \tag{4}$$

In the absence of collisions, the dressed states are separated by Ω, with $E_{\mathrm{II}} > E_{\mathrm{I}}$ for $\Delta < 0$ and $E_{\mathrm{II}} < E_{\mathrm{I}}$ for $\Delta > 0$.

In contrast to the classical-field picture (Fig. 1) in which the only effect of collisions is to shift the energy levels, collisions both shift and couple the dressed states. The amount of the shift of each dressed state is determined by the proportion of bare states it contains. For example, if state $|\mathrm{II}\rangle$ is composed mostly of bare state $|2,n-1\rangle$ then it will shift in the same way as state $|2\rangle$ of Fig. 1. On the other hand if $|\mathrm{II}\rangle$ consists of an almost

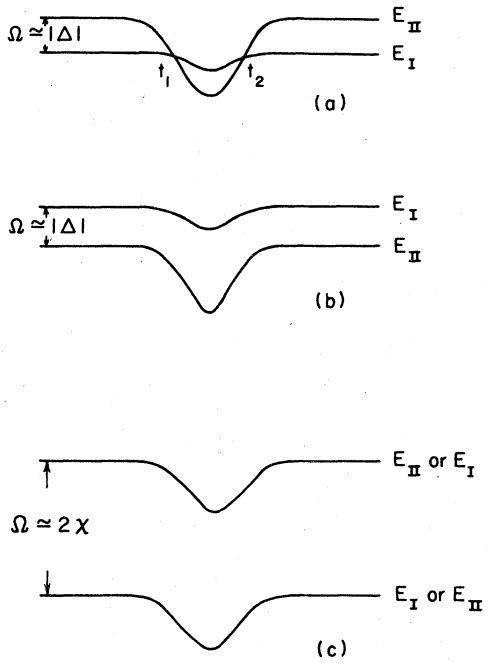

FIG. 2. (a) Variation of the dressed-state energies of a two-level atom during a collision with an attractive potential and red detuning, $\Delta < 0$, in the weak-field limit, $\chi \ll |\Delta|$. The level separation is $\Omega \simeq |\Delta|$; t_1 and t_2 are crossing points corresponding to the two points of instantaneous resonance in Fig. 1. (b) Variation of the dressed-state energies of a two-level atom during a collision with an attractive potential and blue detuning, $\Delta > 0$, in the weak-field limit. No crossing points occur. (c) Variation of the dressed-state energies of a two-level atom during a collision in the high intensity limit, $\chi \gg |\Delta|$. The level separation is $\Omega \approx 2\chi$. If $\Delta < 0$, $E_{II} > E_I$; if $\Delta > 0$, $E_I > E_{II}$. No crossing is possible regardless of the sign of Δ.

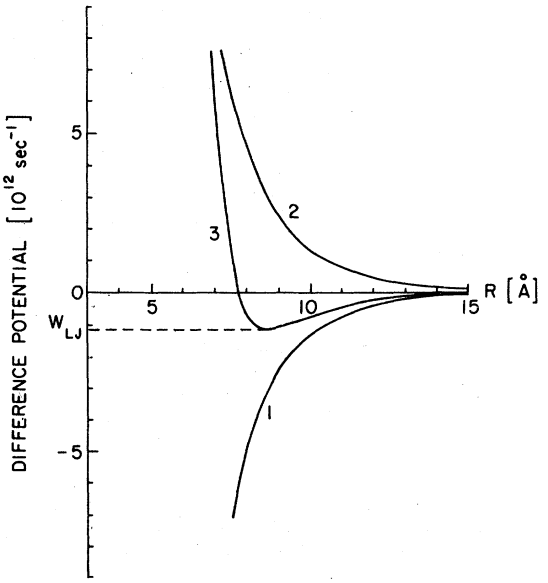

FIG. 3. Interatomic difference potentials. (1) Attractive Van der Waals potential, $C_6^{VDW} = -1.26 \times 10^{18}$ Å^6/sec. (2) Repulsive Van der Waals potential, $C_6^{VDW} = 1.26 \times 10^{18}$ Å^6/sec. (3) Lennard-Jones potential, $C_6^{LJ} = -1.03 \times 10^{18}$ Å^6/sec, $C_{12}^{LJ} = 2.23 \times 10^{23}$ Å^{12}/sec. The well depth is $W_{LJ} = -1.19 \times 10^{12}$ sec^{-1} and occurs at $R = 8.7$ Å.

equal admixture of bare states $|1,n\rangle$ and $|2,n-1\rangle$ it will shift as the average of the shifts of the states $|1\rangle$ and $|2\rangle$ of Fig. 1. The role of collisions on the dressed states is best illucidated by examining the weak- and strong-field limits.

Weak fields—$\chi \ll |\Delta|$. In this limit, state $|\mathrm{II}\rangle$ is separated from state $|\mathrm{I}\rangle$ by Δ [see Eq. (3)] and the dressed states are approximately equal to the bare ones. Consequently the collisional shift of the levels is the same as for the two atomic states. The instantaneous energy levels of the dressed states during a collision are shown in Figs. 2(a) and 2(b) for negative and positive Δ, respectively, assuming an attractive potential. The "instantaneous resonances" of the classical-field picture are transformed into "crossing points" in the dressed-atom approach. As is evident from Figs. 2(a) and 2(b) crossing points can occur for red detunings but will never occur for blue ones.

Strong fields—$\chi \gg |\Delta|$. In the strong-field limit, the dressed states are separated by 2χ and are given by $|\mathrm{I}\rangle$, $|\mathrm{II}\rangle = (1/\sqrt{2})(|1,n\rangle \pm |2,n-1\rangle)$. Since the relative populations of the bare states is the same in each of the dressed states, the collisional shift for the dressed states is identical[25] as shown in Fig. 2(c). Hence the *relative* shift of the dressed states is zero and it is *impossible* to have a crossing, regardless of the sign of Δ, provided $|\Delta| \ll \chi$.

For intermediate-field strengths $\chi \approx |\Delta|$, features of both the weak- and strong-field cases are present.

Since crossings can occur only for the weak-field limit $\chi < |\Delta|$, it is of some interest to determine the *additional* conditions needed to ensure a crossing. A crossing occurs if the collisional level shift equals Δ at some time during the collision [or equivalently, if the applied frequency equals the instantaneous separation $\omega_0(t)$ of the two atomic states]. Instead of using the time t, one can easily as well parametrize the collisional shifts by the internuclear separation R which, in turn, depends on t for a given collision. In Fig. 3 are shown the collisional shifts as a function of internuclear separation for the cases of (1) attractive potential, (2) repulsive potential, (3) Lennard-Jones-type[26] potential.

Crossings occur if there is some $R(t_c)$ during a collision for which Δ equals the collisional shift. Clearly, crossings do *not* occur in case (1) if $\Delta > 0$, in case (2) if $\Delta < 0$ and in case (3) if both $\Delta < 0$ and $|\Delta| > |W_{LJ}|$ ($|W_{LJ}|$ is the well depth of the

Lennard-Jones potential). For all other values of Δ, crossings occur for some range of impact parameters and relative velocities, although rather high relative velocities would be needed to ensure a crossing with repulsive potentials and $\Delta \gtrsim$ thermal energy. If both $\Delta > 0$ and $\Delta < 0$ crossings occur in case (3), the $\Delta > 0$ crossing occurs for a smaller range of impact parameters.

We have not yet indicated the manner in which the presence or absence of crossings affects the absorption cross section. In order to do so, it is convenient to introduce the optical collision impact parameter b_c,[27] defined as the impact parameter for which

$$\int_{-\infty}^{\infty} [\omega_0(t') - \omega_0]\, dt' = 1 .$$

The parameter b_c is the characteristic impact parameter for the weak-field case, producing a change sufficient to significantly disturb the phase of the atomic dipole. The collision time $\tau_c = b_c/v$ and $\omega_c = 1/\tau_c$. The collision interaction possesses frequency components $\omega \lesssim \omega_c$. The importance of crossings then depends on whether $\Omega\tau_c = (\Delta^2 + 4\chi^2)^{1/2}\tau_c \ll 1$ (impact limit) or $\Omega\tau_c > 1$.

If $\Omega\tau_c \ll 1$, the collision possesses sufficient frequency components to compensate for the detuning, i.e., $\omega_c/|\Delta| \gg 1$. In this case, the sign of the detuning is relatively unimportant, indicating that crossing points do not play a significant role in the process. Another way to view this result is as follows: Crossing points are points of stationary phase for the dipole oscillator. Only if the oscillator's phase is rapidly varying in the *absence of collisions* does the point of stationary phase produce the major contribution in the absorption process. In the impact limit $\Omega\tau_c \ll 1$, the phase is *not* rapidly varying in the absence of collisions, and crossings are irrelevant. In the weak-field limit the absorption cross section varies as Δ^{-2} in the impact region.

If $\Omega\tau_c \gg 1$, the oscillator's phase is rapidly varying in the absence of collisions. Collision-induced crossings can greatly enhance the absorption cross section. In the weak-field limit, the absorption cross section will vary as $|\Delta|^{-p}$ $(p > 0)$ if crossings occur and as some power of $|\Delta|$ times $\exp[-\alpha|\Delta\tau_c|^q]$ $(q > 0)$ if no crossings occur.[19-21] This difference in dependence on Δ indicates the importance of crossings when $\Omega\tau_c > 1$. In the strong-field case no crossings occur and the cross section falls as $\exp[-\beta(\chi\tau_c)^{q'}]$ as a function of the field strength.[1] In the above α and β are constants.

In reference to the specific potentials of Fig. 3, general conclusions can be reached:

(i) In the impact limit $\Omega\tau_c \ll 1$, absorption cross sections go as Δ^{-2} for all potentials.
(ii) If $\Omega\tau_c \gtrsim 1$ and $\chi > |\Delta|$, the absorption cross section is approximately independent of $|\Delta|$ for a fixed χ and is an exponentially decreasing function of χ for a fixed Δ.
(iii) If $\Omega\tau_c > 1$ and $|\Delta| > \chi$, the cross sections fall as $|\Delta|^{-p}$ if a crossing occurs ($\Delta < 0$, attractive; $\Delta > 0$, repulsive; $\Delta > 0$, Lennard-Jones; $\Delta < 0$ if also $|\Delta| < |W_{LJ}|$, Lennard-Jones), and as some power of $|\Delta|$ times $\exp(-\alpha|\Delta\tau_c|^q)$ if no crossing occurs. For attractive potentials the profile goes as $|\Delta|^{-p}$ for red detunings and exponentially for blue ones. For repulsive potentials the profile goes as Δ^{-p} for blue detunings and exponentially for red ones. For Lennard-Jones-type potentials, there are two regions. For $|\Delta| < |W_{LJ}|$ for both blue and red detunings the profile has a power-law dependence in $|\Delta|$ (the cross section is larger on the red side since red crosssings occur for a larger range of impact parameters). For $|\Delta| > |W_{LJ}|$, the blue side still goes as a power law in $|\Delta|$, but the red side falls off exponentially. Thus for very large $|\Delta|$, the absorption cross section on the blue side will be larger than that on the red.

These features will be verified by the numerical calculations of Secs. III and IV. One can conclude that, if $|\Delta|\tau_c > 1$, the optimum external field strength to use for CARE as $\chi \approx |\Delta|$, since higher fields give an exponential falloff in the cross section.

III. EQUATIONS OF MOTION

The Hamiltonian for a two-level active atom interacting with a radiation field and a perturber atom can be written as

$$H = H_A + H_R + H_{AR} + V(t) = H_0 + V(t), \tag{5}$$

where (i) the free atomic Hamiltonian H_A has two eigenstates $|1\rangle, |2\rangle$, with eigenenergies $E_1, E_2; E_2 - E_1 = \omega_0$; (ii) $H_R = \omega a^\dagger a$ is the quantized free-field Hamiltonian describing a single-mode field with ω the photon energy; (iii) the active-atom-field interaction is given in the rotating-wave approximation by $H_{AR} = \chi'(aR^+ + a^\dagger R)$, where a and $a^\dagger$ are the usual annihilation and creation operators, respectively, for photons of frequency ω, R^+ and R are the raising and lowering operators for the two atomic states, and χ' is the coupling constant, defined by $\chi = \sqrt{n}\chi'$ with n the number of photons; (iv) the effective interaction with the perturber $V(t)$ is taken to be time dependent since the internuclear motion is not quantized, and is diagonal in the basis of bare states $|1, n\rangle$, $|2, n-1\rangle$ (eigenstates of $H_A + H_R$),

$$V_1(t)=\langle 1,n|V(t)|1,n\rangle\,,$$
$$V_2(t)=\langle 2,n-1|V(t)|2,n-1\rangle\,, \tag{6}$$
$$\langle 1,n|V(t)|2,n-1\rangle=\langle 2,n-1|V(t)|1,n\rangle=0\,,$$

owing to the absence of inelastic collisions. This is in general a good approximation for electronic and vibrational transitions where the thermal energy is not high enough to excite the atom.

The calculation is carried out in a dressed-state basis composed of the eigenstates, $|\mathrm{I}\rangle$, $|\mathrm{II}\rangle$ of $H_0=H_A+H_R+H_{AR}$ given in Eq. (2). Defining

$$V_S(t)=V_1(t)+V_2(t);\quad V_d(t)=V_2(t)-V_1(t) \tag{7}$$

writing

$$|\psi\rangle=[C_{\mathrm{I}}(t)|\mathrm{I}\rangle+C_{\mathrm{II}}(t)|\mathrm{II}\rangle]\,\exp\left(-\frac{1}{2}i\int_{-\infty}^{t}V_S(t')\,dt'\right)$$

and using the Schrödinger equation together with Eqs. (2), (3), and (6), we obtain the equations for the probability amplitudes

$$i\dot{C}_{\mathrm{I}}=[E_{\mathrm{I}}-(\Delta/2\Omega)V_d(t)]C_{\mathrm{I}}+\chi/\Omega\;V_d(t)C_{\mathrm{II}}\,,$$
$$i\dot{C}_{\mathrm{II}}=\chi/\Omega\;V_d(t)C_{\mathrm{I}}+[E_{\mathrm{II}}+(\Delta/2\Omega)V_d(t)]C_{\mathrm{II}}\,. \tag{8}$$

In the dressed basis, $V(t)$ is no longer diagonal; C_{I} and C_{II} are coupled through off-diagonal matrix elements which are nonzero only during a collision. This makes the dressed-state basis a favorable choice in numerical calculations, since we can limit the integration within the short range of a collision. If $C_{\mathrm{I}}(t=-\infty)=1$ and $|\Delta|\times$(radiation pulse rise time)>1 (as is implicitly assumed throughout this work), C_{II} goes to zero as $t\to+\infty$ in the absence of collisions. Thus, $|C_{\mathrm{II}}(t=\infty)|^2$ represents the contribution of CARE. Note that the probabilities $|C_{\mathrm{I}}|^2$, $|C_{\mathrm{II}}|^2$ depend only on the difference potential.

To solve Eqs. (7), we assume that the atoms follow straight-line trajectories and take two model potentials, an attractive Van der Waals potential

$$V_d^{\mathrm{VDW}}(t)=C_6^{\mathrm{VDW}}/(b^2+v^2t^2)^3 \tag{9}$$

with $C_6^{\mathrm{VDW}}<0$ an effective Van der Waals constant, and a Lennard-Jones potential

$$V_d^{\mathrm{LJ}}(t)=\frac{C_6^{\mathrm{LJ}}}{(b^2+v^2t^2)^3}+\frac{C_{12}^{\mathrm{LJ}}}{(b^2+v^2t^2)^6} \tag{10}$$

with $C_{12}^{\mathrm{LJ}}>0$. In Eqs. (9) and (10), b is the impact parameter and the point of closest approach is taken at $t=0$.

All relaxation rates are neglected in Eq. (8) owing to conditions (1). As discussed in the Introduction, it suffices to consider a single collision with impact parameter b and relative velocity v. The total CARE cross section is given by

$$\sigma=2\pi\int_0^\infty|C_{\mathrm{II}}(b,\infty)|^2 b\,db\,. \tag{11}$$

No average over the velocity will be attempted.

For a Hamiltonian that is an even function of time, one can show[28] that

$$C_{\mathrm{II}}(t)C_{\mathrm{I}}^*(-t)-C_{\mathrm{I}}(t)C_{\mathrm{II}}^*(-t)=C_{\mathrm{II}}(0)C_{\mathrm{I}}^*(0)-C_{\mathrm{I}}(0)C_{\mathrm{II}}^*(0)\,, \tag{12}$$
$$C_{\mathrm{I}}(t)C_{\mathrm{I}}(-t)+C_{\mathrm{II}}(t)C_{\mathrm{II}}(-t)=C_{\mathrm{I}}^2(0)+C_{\mathrm{II}}^2(0)\,.$$

In addition, unitarity is maintained,

$$|C_{\mathrm{I}}(t)|^2+|C_{\mathrm{II}}(t)|^2=1\,. \tag{13}$$

Since the integration of Eqs. (8) can be very time consuming, Eqs. (12) and (13) can be used to reduce the range of integration to $-\infty<t\leq 0$. The integration is conveniently done using a subroutine called DVERK in IMSL which uses a Runga-Kutta method based on Verner's fifth- and sixth-order formulas.[29]

IV. RESULTS

A. Van der Waals potential

In the following, the Van der Waals constant C_6^{VDW} is taken to be -1.26×10^{18} Å^6/sec and $v=10^5$ cm/sec.

1. Weak-field case, χ $|\Delta|$

The variation of the probability $|C_{\mathrm{II}}(b,\infty)|^2$ as a function of impact parameter b is represented in Fig. 4(a) for red detuning and Fig. 4(b) for blue detuning for values $\chi=10^8$ sec^{-1}, $|\Delta|=5\times10^{11}$ sec^{-1}. The probability $|C_{\mathrm{II}}(b,\infty)|^2$ is an oscillating function of b with an envelope increasing with increasing b on the red side and decreasing with increasing b on the blue side. The oscillations start at some finite b and get faster as b is decreased. The results at this low detuning, $|\Delta|\tau_c\simeq 0.5$, can be compared with the impact approximation ($|\Delta|\tau_c\ll 1$). In the impact approximation, the equations are easily solved to yield the standard result of impact pressure-broadening theory,

$$|C_{\mathrm{II}}(b,\infty)|^2=P(b)=(2\chi^2/\Delta^2)(1-\cos\theta) \tag{14}$$

with

$$\theta=\int_{-\infty}^{\infty}\frac{C_6^{\mathrm{VDW}}}{(b^2+v^2t^2)^3}\,dt=\frac{3\pi C_6^{\mathrm{VDW}}}{8b^5v}\,. \tag{15}$$

For the parameters chosen, $P(b)$ oscillates at a constant amplitude 0.16×10^{-6}, irrespective of blue or red detuning. The impact approximation underestimates the transition probability on the red side, overestimates it on the blue side, but still provides a fair approximation at this detuning. For detunings $|\Delta|\tau_c<1$ the presence of crossings is

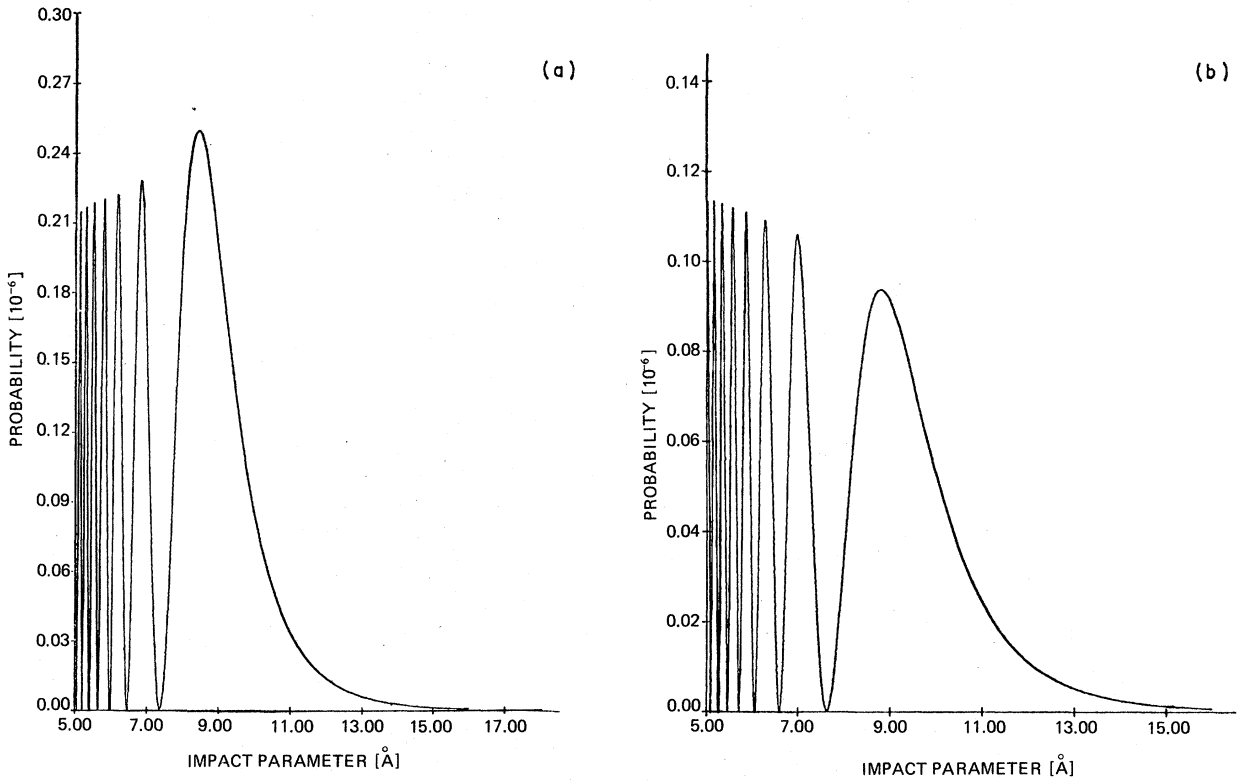

FIG. 4. (a) The probability $|C_{II}(b,\infty)|^2$ as a function of impact parameter b for the attractive Van der Walls potential and small red detuning. $\chi = 10^8$ sec^{-1} ($\chi\tau_c = 1.08\times10^{-4} \ll 1$), $C_6^{VDW} = -1.26\times10^{18}$ Å^6/sec, $v = 10^5$ cm/sec, $\Delta = -5\times10^{11}$ sec^{-1} ($|\Delta|\tau_c = 0.54 < 1$). (b) The probability as a function of impact parameter for the attractive Van der Walls potential and small blue detuning, $\Delta = 5\times10^{11}$ sec^{-1} ($\Delta\tau_c = 0.54 < 1$). Other parameters are the same as those in Fig. 4 (a).

seen to be relatively unimportant, as predicted in Sec. II.

The behavior of $|C_{II}(b,\infty)|^2$ for larger detunings $|\Delta|\tau_c > 1$ is shown in Figs. 5(a) and 5(b) for $|\Delta| = 6\times10^{12}$ sec^{-1}, $\chi = 10^8$ sec^{-1}. On the red side, the probability envelope is considerably greater than the impact value 0.11×10^{-8}. Crossings provide stationary phase points to eliminate some of the rapid oscillations owing to large $|\Delta|$. The maximum contribution is centered about the largest b giving rise to a crossing in agreement with calculations using a uniform approximation[30] that consider this region. On the blue side, the rapid phase variation due to detuning further diminishes the probability from its impact value. On both sides, the positions of maxima are shifted to smaller impact parameters, since higher-frequency components (consequently smaller b) are needed to compensate for larger $|\Delta|$. In this range of detuning, the crossing point on the red side greatly enhances the cross section relative to that on the blue, in agreement with the discussion of Sec. II.

The oscillation of $|C_{II}(b,\infty)|^2$ has been interpreted as the phased cancellation or enhancement of the transition amplitudes from the incoming and outgoing crossings during the collision. This interpretation is applicable only for large detunings on the red side. It is not an appropriate interpretation on the blue side where no crossings occur nor for detunings $|\Delta|\tau_c < 1$ where crossing points do not provide the major contributions to the absorption.

Equation (11) is integrated numerically from a given impact parameter, $b_0 = 5$ Å say, to infinity, and the contribution from 0 to b_0 is estimated. The region of small b is particularly troublesome owing to the fast oscillations involved. Fortunately, the contribution from small impact parameters is relatively unimportant owing to the nature of the envelope function and to the weighting factor $b\,db$.

A line profile is shown in Fig. 6 and is in agreement with the qualitative discussion of Sec. II. For small detunings, $|\Delta|\tau_c \ll 1$, the cross section falls off as Δ^{-2} on both the red and the blue sides. For large detunings, $|\Delta|\tau_c \gg 1$ on the red side, it falls off as $|\Delta|^{-3/2}$ in agreement with the quasistatic results of classical pressure-broadening theor-

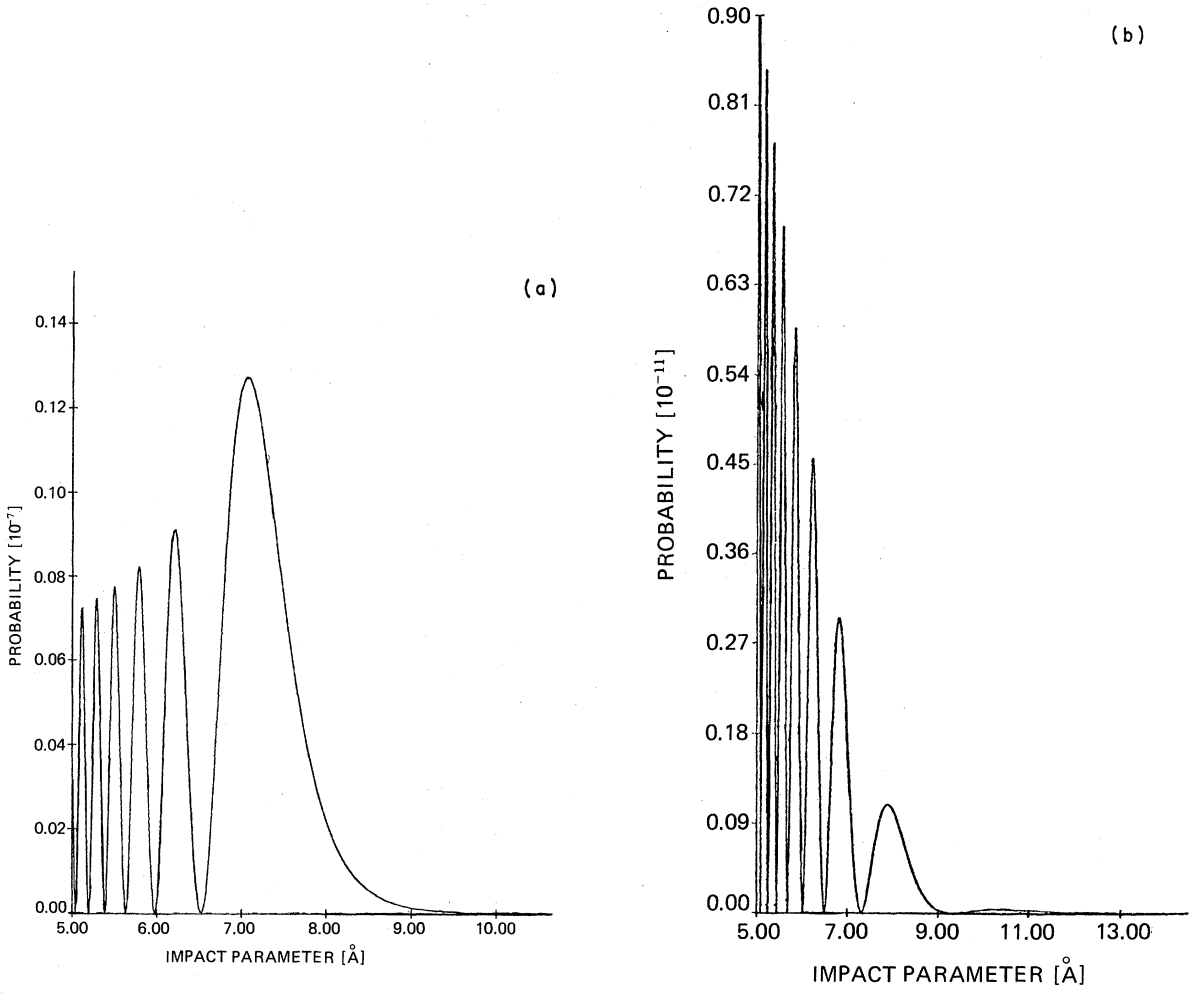

FIG. 5. (a) Probability as a function of impact parameter for the attractive Van der Waals potential and a large red detuning. $\chi = 10^8\,\mathrm{sec}^{-1}$, $C_6^{\mathrm{VDW}} = -1.26\times10^{18}\,\text{Å}^6/\mathrm{sec}$, $v = 10^5\,\mathrm{cm/sec}$, $\Delta = -6\times10^{12}\,\mathrm{sec}^{-1}$ ($|\Delta|\tau_c = 6.49 > 1$). (b) The probability as a function of impact parameter for the attractive Van der Waals potential for a large blue detuning $\Delta = 6\times10^{12}\,\mathrm{sec}^{-1}$ ($\Delta\tau_c = 6.49 > 1$). Other parameters are the same as in Fig. 5 (a).

ies.[19-21] On the blue side, the cross section goes approximately as $\Delta^{-7/3}\exp(-\alpha\Delta^{5/6})$ with α a constant. This has the same Δ dependence as the asymptotic results of Tvorogov and Fomin,[31] although their results differ from ours by a multiplicative factor. The results of Vainshtein *et al.*[32] are also shown in Fig. 6, and are seen to differ from our results in both their absolute magnitude and Δ dependence.

2. *Intense-field case* $|\Delta| \gg \chi$

There is no additional difficulty in numerically integrating Eqs. (8) in the case of strong fields. As discussed in Sec. II, there are no crossings if $\chi \ll |\Delta|$. For $\chi\tau_c < 1$, the criteria for the impact limit are satisfied and one obtains the results of impact limit; for $\chi\tau_c > 1$, absorption cross sections are expected to be exponentially small (in the factor $\chi\tau_c$) in both the blue and red wings, owing to the absence of crossings.

The numerical results confirm these conclusions. For $\chi\tau_c < 1$, the probability $|C_{II}(b,\infty)|^2$ is an oscillating function in b with constant amplitudes (impact results), while for $\chi\tau_c \gg 1$, it has the characteristic shapes shown in Figs. 4(b) and 5(b), indicating the absence of a crossing irrespective of the sign of the detuning. For $\chi\tau_c \ll 1$ and $|\Delta| < \chi$, the impact theory is valid and one obtains a symmetric absorption profile with a Δ^{-2} dependence.

3. $\sigma(\Delta)$ *for* $\chi\tau_C \gtrsim 1$

One can combine Secs. IV A 1 and IV A 2 to obtain the spectrum for $\chi\tau_c \gtrsim 1$, and a typical spectrum is shown in Fig. 7. For $|\Delta| \ll \chi$, there are no cross-

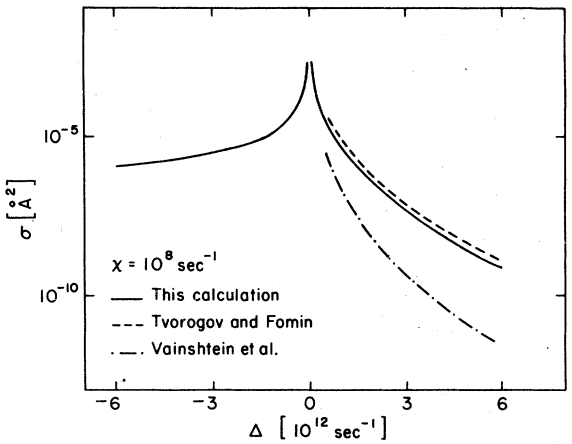

FIG. 6. Absorption cross section $\sigma(\Delta)$ for an attractive Van der Waals potential in the weak-field limit with parameters as in Figs. 4—, this calculation;---, Tvorogov and Fomin (Ref. 21); – – – –, Vainshtein *et al.* (Ref. 32).

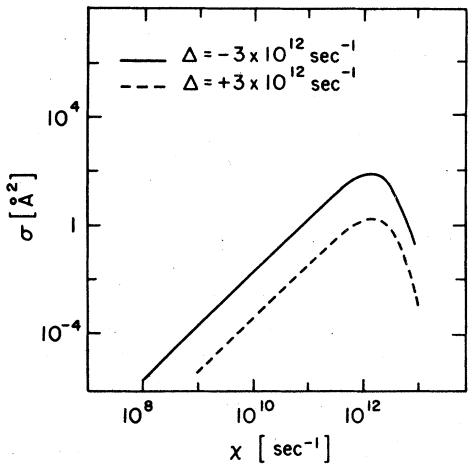

FIG. 8. Absorption cross section $\sigma(\chi)$ for the attractive Van der Waals potential with a fixed detuning $|\Delta| = 3\times10^{12}$ sec^{-1}. Other parameters are the same as in Fig. 5. Solid line, red detuning; dashed line, blue detuning.

ings and the absorption cross section is approximately constant with $|\Delta|$. For $|\Delta| \gg \chi$, one regains the limiting condition of Sec. IV A 1 with the corresponding line wings decreasing as $|\Delta|^{-3/2}$ on the red side and as $\Delta^{-7/3}\exp(-\alpha\Delta^{5/6})$ on the blue side. On the red side the profile passes through a maximum at $|\Delta| \approx \chi$, indicating the transition from the no-crossing ($\chi > |\Delta|$) to the crossing ($\chi < |\Delta|$) case. On the blue side, the falloff is monotonic owing to the monotonically increasing separation of the dressed-state energies with increasing Δ.

For a given χ, maximum excitation is achieved for a red detuning of $|\Delta| \approx \chi$.

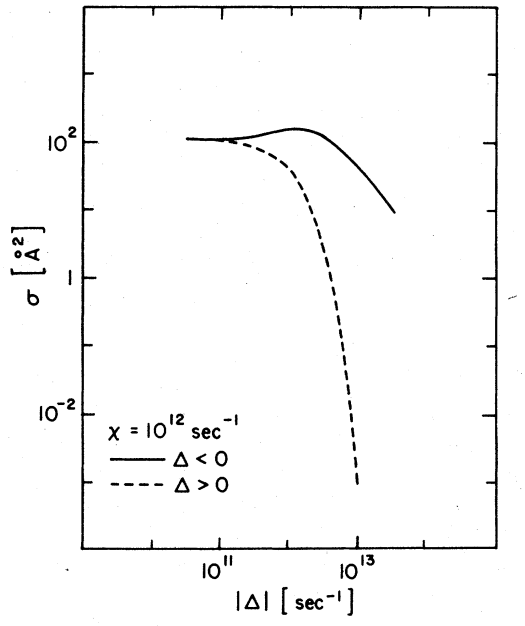

FIG. 7. Absorption cross section $\sigma(\Delta)$ at a high intensity, $\chi = 10^{12}$ sec^{-1} ($\chi\tau_c = 1.08 \gtrsim 1$), for the attractive Van der Waals potential. Other parameters are the same as in Figs. 5. Solid line, red detuning: dashed line, blue detuning.

4. $\sigma(\chi)$ *for fixed* $|\Delta|$

The absorption cross section as a function of χ for fixed $|\Delta|$ is shown in Fig. 8. The cross section varies as χ^2 in both the red and blue wings provided either $\chi\tau_c \ll 1$ or $\chi \ll |\Delta|$. However, for field strengths $\chi \gg |\Delta|$ and $\chi\tau_c > 1$ saturation occurs and the cross sections fall off approximately as $\exp(-\beta\chi^{5/6})$ consistent with the result of Lisitsa and Yakovlenko.[1] At these large-field strengths, the dressed states never cross [Fig. 2(c)] and their separation is dominated by χ rather than $|\Delta|$. This saturation effect is not at all related to unitarity, since it has been implicitly assumed that the excited-state probability remains small in comparison with unity. The saturation mechanism is simply the one discussed in connection with Fig. 2(c) of Sec. II.

B. Lennard-Jones potential

The difference potential shown in Fig. 3 is plotted with $C_6^{LJ} = -1.03\times10^{18}$ Å^6/sec, $C_{12}^{LJ} = 2.23\times10^{23}$ Å^{12}/sec, which are given by Kielkopf *et al.*[33] for cesium $6S_{1/2}$-$7P_{1/2}$ transition perturbed by Xe.

1. *Weak-field case,* $\chi \ll |\Delta|$

Figure 9 shows $|C_{II}(b,\infty)|^2$ as a function of b, with $|\Delta| = 3\times10^{10}$ sec^{-1}, $\chi = 10^9$ sec^{-1}. At this detuning, the impact approximation is very good.

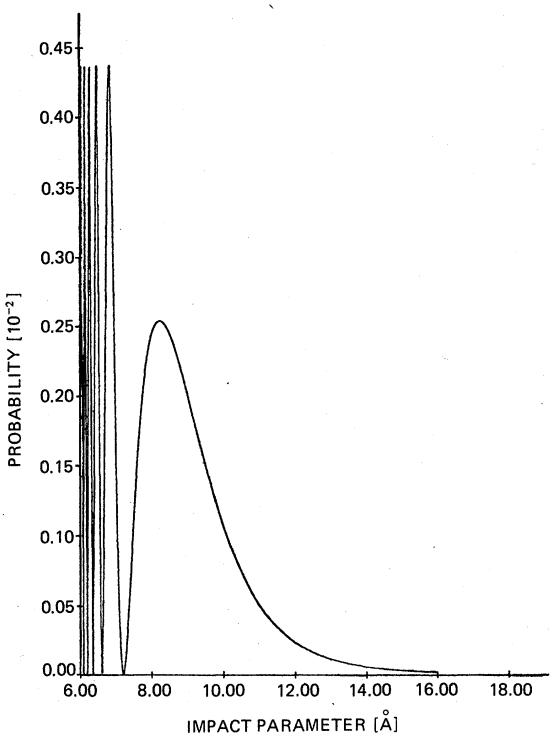

FIG. 9. Probability as a function of impact parameter b for the Lennard-Jones potential. $\chi = 10^9$ sec^{-1} ($\chi\tau_c = 1.02\times10^{-3} \ll 1$), $\Delta = 3\times10^{10}$ sec^{-1} ($\Delta\tau_c = 3.06\times10^{-2} \ll 1$), $v = 10^5$cm/sec, $C_6^{LJ} = -1.03\times10^{18}$ Å^6/sec, $C_{12}^{LJ} = 2.23\times10^{23}$Å^{12}/sec.

One can see oscillations with constant amplitude (except for one additional peak at $b = 8.24$ Å) with positions of maxima (and minima) and their heights matched by the results of the impact approximation. The extra peak is characteristic of Lennard-Jones potentials. The impact phase for a Lennard-Jones potential is

$$\theta_{LJ} = \int_{-\infty}^{\infty}\left(\frac{C_6^{LJ}}{(b^2+v^2t^2)^3} + \frac{C_{12}^{LJ}}{(b^2+v^2t^2)^6}\right)dt = \frac{3\pi C_6^{LJ}}{8b^5v} + \frac{63\pi C_{12}^{LJ}}{256b^{11}v}\,. \tag{16}$$

In addition to $b=\infty$, $\theta_{LJ}=0$ at $b_1 = (-\frac{21}{32}C_{12}^{LJ}/C_6^{LJ})^{1/6}$. Since the minima of $|C_{II}(b,\infty)|^2$ are determined by $\theta_{LJ} = 2n\pi$, $n = 0, 1, 2, \ldots$, in the impact region, the extra zero results in an additional peak with its height determined by the maximum phase $|\theta_{LJ}|$ in the interval (b_1, ∞).

For larger red detunings, $|C_{II}(b,\infty)|^2$ follows a typical crossing behavior [Figs. 4(a) and 5(a)] if $|\Delta| < |W_{LJ}|$ and noncrossing behavior [Figs. 4(b) and 5(b)] if $|\Delta| > |W_{LJ}|$ in agreement with the discussion of Sec. II. There is always a crossing on the blue side, regardless of detuning, and $|C_{II}(b,\infty)|^2$ displays the type of crossing behavior shown in Figs. 4(a) and 5(a).

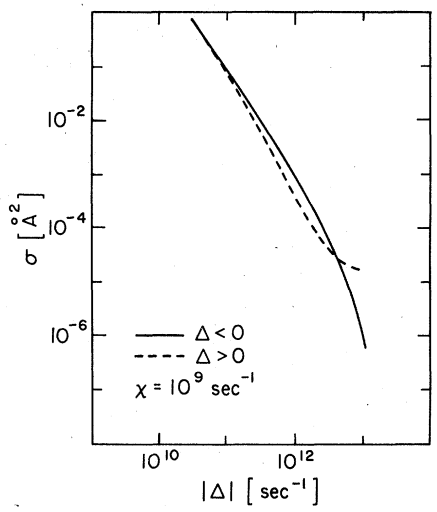

FIG. 10. $\sigma(\Delta)$ for a Lennard-Jones potential in the weak-field limit, $\chi = 10^9$ sec^{-1} ($\chi\tau_c = 1.02\times10^{-3} \ll 1$). Other parameters are the same as in Fig. 9. Solid line, red detuning; dashed line, blue detuning.

The absorption profile is shown in Fig. 10 for $\chi = 10^9$ sec^{-1}. At detunings $< 10^{11}$ sec^{-1}, the impact approximation is valid and absorption falls as $|\Delta|^{-2}$. For $|\Delta|\tau_c \gtrsim 1$, but $|\Delta| < |W_{LJ}|$ there are crossings for both red and blue detunings. Excitation is greater for red than blue detunings, owing to the larger range of impact parameters giving rise to the crossings on the red side as discussed in Sec. II. As $|\Delta|$ is further increased such that $|\Delta| > |W_{LJ}|$, there is no longer a crossing for red detunings and the red wing begins to fall off rapidly. The change in dependence from power law to exponential falloff with detuning on the red side is the well known satellite feature of potentials possessing minima. For blue detuning, the $|\Delta|$ dependence approaches $|\Delta|^{-1.25}$, typical for the far wings of a power-law potential going as R^{-12}. For large $|\Delta|$, the blue wing eventually exceeds red wing absorption. The line shape has the same qualitative features observed by Carlsten *et al.*[11] in a Sr-Ar system. The results differ quantitatively in the specific $|\Delta|$ dependence of the cross sections as well as in the ratio of red to blue absorption for a given $|\Delta|$. These discrepancies may be attributed to differences between the Ar-Sr and Cs-Xe interatomic potentials.

2. $\sigma(\Delta)$ for $\chi\tau_c \gtrsim 1$

A profile $\sigma(\Delta)$ for $\chi = 10^{12}$ sec^{-1} is shown in Fig. 11. Since $\chi\tau_c \gtrsim 1$, the presence or absence of crossing greatly affects the magnitude of the absorption cross section. For $|\Delta| \ll \chi$, the dressed states of Fig. 2(c) do not cross and the cross sec-

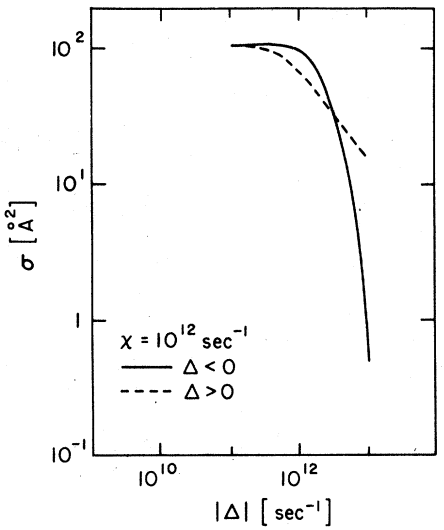

FIG. 11. $\sigma(\Delta)$ at a high intensity, $\chi = 10^{12}$ sec^{-1} ($\chi\tau_c = 1.02 \gtrsim 1$), for the Lennard-Jones potential. Other parameters are the same as in Fig. 9. Solid line, red detuning; dashed line, blue detuning.

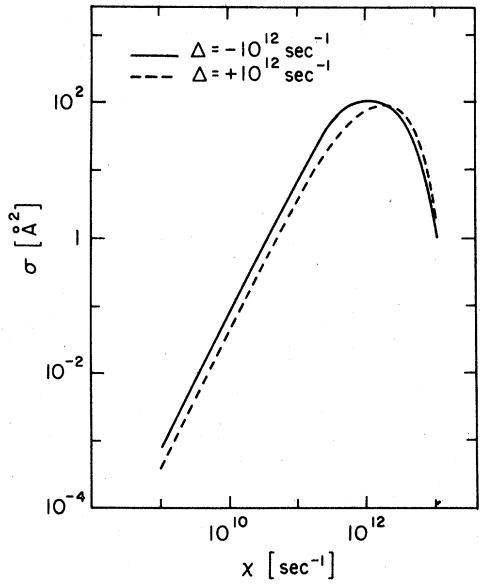

FIG. 12. $\sigma(\chi)$ for the Lennard-Jones potential with $|\Delta| = 10^{12}$sec^{-1} ($|\Delta|\tau_c = 1.02 \gtrsim 1$). Other parameters are the same as in Fig. 9. Solid line, red detuning; dashed line, blue detuning. Saturation occurs at lower χ for the red wing than for the blue.

tions for both red and blue detunings are approximately independent of Δ. For $|\Delta| \gtrsim \chi$ and $|\Delta| < |W_{LJ}|$, a crossing becomes possible on the red wing (since the χ chosen is less than $|W_{LJ}|$) and also on the blue wing. For the parameters chosen, the red wing increases slightly with increasing $|\Delta|$, owing to the presence of the crossing, but then begins to decrease exponentially as soon as $|\Delta| > |W_{LJ}|$. The blue wing decreases monotonically with increasing $|\Delta|$, asymptotically going as $|\Delta| |\Delta|^{-1.25}$.

If a value $\chi > |W_{LJ}|$ is chosen, there is never a crossing for red detunings and the red wing decreases monotonically. Figure 11 is consistent with the qualitative discussion of Sec. II. For a given χ, the optimal detuning for maximum excitation depends on the detailed nature of the potential.

3. $\sigma(\chi)$ *for fixed* $|\Delta|$

Finally, the line shape as a function of χ for fixed detuning, $|\Delta| = 10^{12}$ sec^{-1}, is shown in Fig. 12. For $\chi\tau_c \ll |\Delta|\tau_c \approx 1$, the absorption goes as χ^2. There are crossings in both the red and blue wings since $|\Delta| < |W_{LJ}|$. As χ increases, the red crossing disappears at $\chi \simeq \frac{1}{2}(W_{LJ}^2 - \Delta^2)^{1/2}$ and the blue wing crossing disappears at $\chi \simeq \Delta$. The corresponding saturation of the spectrum is clearly seen in Fig. 12, with $\sigma(\chi)$ saturating at smaller χ in the red wing than the blue.

V. SUMMARY

A physical picture of collisionally aided radiative excitation (or emission) (CARE) has been given using a dressed-atom approach. This approach enabled us to obtain general predictions for both the detuning and field dependence of CARE. These predictions were compared with numerical solutions of the problem and were found to successfully explain the CARE line shape. Moreover, the results for a Lennard-Jones potential are qualitatively in agreement with the experimental data of Carlsten *et al.*[11]

The numerical solutions, while costly, offer a much wider range of validity than the asymptotic formulas obtained by previous authors. Our methods can easily be extended to problems with arbitrary interatomic potentials and to other than straight-line internuclear paths.

ACKNOWLEDGMENTS

This work was supported by the U. S. ONR through Contract No. N00014-77-C-0553, and computational time was supported in part by DOE under Contract No. E(11-1)-3077 at N. Y. U. and by the N. Y. U. Computer Center.

[1]V. S. Lisitsa and S. I. Yakovlenko, Sov. Phys. JETP 39, 759 (1974); 41, 233 (1975); S. P. Andreev and V. S. Lisitsa, *ibid.* 45, 38 (1977).
[2]A. M. F. Lau, Phys. Rev. A 13, 139 (1976); N. M. Kroll and K. M. Watson, Phys. Rev. A 13, 1018 (1976).
[3]W. H. Miller and T. F. George, J. Chem. Phys. 56, 5637 (1972); J. M. Yuan, J. R. Liang, and T. F. George, *ibid.* 66, 1107 (1977).
[4]P. R. Berman, in *Advances in Atomic and Molecular Physics*, edited by D. R. Bates and B. Bederson, (Academic, New York, 1977), Vol. 13, p. 57–112.
[5]M. G. Payne and M. H. Nayfeh, Phys. Rev. A 13, 596 (1976); M. H. Nayfeh and M. G. Payne, *ibid.* 17, 1695 (1978); M. G. Payne, C. W. Choi, and M. H. Nayfeh (unpublished).
[6]R. W. Falcone, W. R. Green, J. C. White, J. F. Young, and S. E. Harris, Phys. Rev. A 15, 1333 (1976); S. E. Harris and J. C. White, IEEE J. of Quantum Electron. QE-13, 972 (1977).
[7]Ph. Cahuzac and P. E. Toschek, Phys. Rev. Lett. 40, 1087 (1978).
[8]L. I. Gudzenko and S. I. Yakovlenko, Sov. Phys. JETP 35, 877 (1972).
[9]S. Geltman, J. Phys. B 10, 3057 (1977).
[10]P. Milonni, J. Chem. Phys. 66, 3715 (1977).
[11]J. L. Carlsten, A. Szöke, and M. G. Raymer, Phys. Rev. A 15, 1029 (1977).
[12]A. Omont, E. W. Smith, and J. Cooper, Astrophys. J. 175, 185 (1972); J. Cooper and R. J. Ballagh (unpublished).
[13]G. Nienhuis and F. Schuller, Physica C 92, 397 (1977).
[14]A. Ben-Reuven, J. Jortner, L. Klein, and S. Mukamel, Phys. Rev. A 13, 1402 (1976).
[15]A. Gallagher and T. Holstein, Phys. Rev. A 16, 2413 (1977).
[16]D. Grischkowsky, Phys. Rev. A 7, 2096 (1973).
[17]For an extensive list of papers, books, and reviews, see P. R. Berman, Appl. Phys. 6, 283 (1975).
[18]E. Lindholm, Ark. Mat. Astron. Fys. A 32, 1 (1945).
[19]P. W. Anderson, Phys. Rev. 86, 809 (1952); P. W. Anderson and J. D. Talman, Rep. Bell Tel. Labs. (unpublished).
[20]J. Szudy and W. E. Baylis, J. Quant. Spectrosc. Radiat. Transfer 15, 641 (1975).
[21]S. D. Tvorogov and V. V. Fomin, Opt. Spectrosc. 30, 228 (1971).
[22]J. Kielkopf, J. Phys. B 9, 1601 (1976); 11, 25 (1978).
[23]K. M. Sando and J. C. Wormhoult, Phys. Rev. A 7, 1889 (1973).
[24]C. Cohen-Tannoudji, *Cargèse Lecture in Physics* (Gordon and Breach, New York, 1968), Vol. 2, p. 347.
[25]The velocity-changing effects are neglected throughout the calculation so that this picture is valid.
[26]A. Lennard-Jones potential is used because of its mathematical simplicity. For more realistic potentials, see W. E. Baylis, J. Chem. Phys. 51, 2665 (1969); J. Pascale and J. Vandeplanque, *ibid.* 60, 2278 (1974).
[27]This was originally defined by V. Weisskopf, sometimes referred to as the Weisskopf radius.
[28]C. F. Lebeda and W. R. Thorson, Can. J. Phys. 48, 2937 (1970).
[29]T. E. Hull, W. H. Enright, and K. R. Jackson, TR No. 100, Dept. of Computer Science, Univ. of Toronto, Oct. 1976.
[30]W. Fritsch and U. Wille, J. Phys. B 11, L43 (1978). For a detailed account of the uniform approximation, see M. S. Child, *Molecular Collision Theory* (Academic, London, 1974), p. 191–194.
[31]Equation (25) of Ref. 21.
[32]Equations (30) and (31) in L. Vainshtein, L. Presnyakov, and I. Sobelman, Sov. Phys. JETP 16, 370 (1963). In this paper, the authors studied a different problem, however, the integral they obtained [Eq. (A1)] took the same form as an integral obtained in a perturbation calculation for the CARE problem.
[33]J. F. Kielkopf, J. E. Davis, and J. A. Gwinn, J. Chem. Phys. 53, 2605 (1970).